coatings

MDPI

Article

About Gas Barrier Performance and Recyclability of Waterborne Coatings on Paperboard

Sterre Bakker [1], Joey Kloos [2], Gerald A. Metselaar [3], A. Catarina C. Esteves [4] and Albert P. H. J. Schenning [1,*]

[1] Laboratory of Stimuli-Responsive Functional Materials and Devices, Department of Chemical Engineering and Chemistry, Eindhoven University of Technology, P.O. Box 513, 5600 MB Eindhoven, The Netherlands
[2] Membrane Materials and Processes, Department of Chemical Engineering and Chemistry, Eindhoven University of Technology, P.O. Box 513, 5600 MB Eindhoven, The Netherlands
[3] BASF Nederland B.V., Innovatielaan 1, 8447 SN Heerenveen, The Netherlands
[4] Laboratory of Physical Chemistry, Department of Chemical Engineering and Chemistry, Eindhoven University of Technology, P.O. Box 513, 5600 MB Eindhoven, The Netherlands
* Correspondence: a.p.h.j.schenning@tue.nl

Abstract: For preserving food packed in environmentally friendly and recyclable paperboard packages, it is important to have sufficient gas barrier performance of the paperboard container. Paperboard has poor intrinsic barrier properties and to overcome this deficiency, so a barrier coating is needed that does not hinder the recycling of the paperboard substrate. However, the gas barrier properties and the recyclability of such coatings have been rarely studied. Here, both the gas barrier performance and the removal of an alkali-soluble resin (ASR)-stabilized waterborne barrier coatings from paperboard are investigated. For barriers for gases, such as nitrogen, carbon dioxide, and oxygen, defect-free coatings are needed which is achieved by applying three coating layers. The oxygen transmission rate (OTR) of the three-layered coating on paperboard was 920 $cm^3/(m^2 \cdot day)$. For water vapor barriers, two coating layers already show a strong improvement, as water follows a different penetration mechanism than the other tested gases. The water vapor transmission rate WVTR of double coated paperboard was 240 $g/(m^2 \cdot day)$. Preliminary results show that the coating is removed by immersion of the coated paperboard in an aqueous alkaline solution at room temperature. This causes de-protonation of the carboxylic acids of the ASR and subsequent re-dispersion of the coating in water. Removing double-layer coatings from the paperboard is more challenging, possibly due to the coating/coating interface between the two coating layers and enhanced adhesion between coating and paperboard.

Keywords: waterborne coating; paperboard; gas barrier; alkali-soluble resin; recycle; aqueous dispersion

Citation: Bakker, S.; Kloos, J.; Metselaar, G.A.; Esteves, A.C.C.; Schenning, A.P.H.J. About Gas Barrier Performance and Recyclability of Waterborne Coatings on Paperboard. *Coatings* **2022**, *12*, 1841. https://doi.org/10.3390/coatings12121841

Academic Editor: Isabel Coelhoso

Received: 1 November 2022
Accepted: 23 November 2022
Published: 28 November 2022

1. Introduction

Food packaging is used to contain and protect food from environmental influences like oxygen (O_2) and water (H_2O). Oxygen has a negative effect on packed food by promoting the growth of microorganisms, causing stale odor, loss of vitamin C, and loss of aroma due to oxidation [1,2]. Therefore, it is important to prevent oxygen from permeating from the environment into the package. Dry and crispy food, like cereals, loses its crunchiness with increasing moisture content [3]. For packed beverages, on the other hand, water must be contained inside the package. Hence, a barrier is needed for both water vapor and liquid water. Another approach to increase the shelf-life of food is by packing the food in a modified atmosphere. The gaseous atmosphere inside the package is changed to an atmosphere that promotes the preservation of food. The main gases used in modified atmospheres are nitrogen (N_2) and carbon dioxide (CO_2) [4,5]. For this reason, these gases need to be contained inside the food container. Moderate vacuum packaging is a packaging technique that is used to reduce the air pressure inside the container and slow down the

metabolism and growth of microorganisms [4]. In this case, the atmospheric gases need to be prevented from entering the reduced-pressure food packaging.

Paperboard is a bio-based and environmentally friendly food packaging material, and for this reason is the most used material, responsible for 40% to 50% of the packaging market [6–8]. Paperboard alone has insufficient barrier properties, so barrier coatings are necessary. The barrier layer must be impermeable to migrants, such as water (vapor), oil and oxygen [9,10]. This layer should not hinder the recycling of paperboard, as more than 80% of paper food packaging waste is recycled in the EU [11]. Recycling of paper starts with pulping, where paper is separated into fibers and the ink is detached from the fibers [12–14]. The main challenge of paper recycling is the removal of non-paper materials, including coatings, adhesives, and inks from the paper. If there is incomplete removal, these contaminations may end up in the recycled paper food packaging and possibly migrate into the food itself, which can be hazardous. With increased recycling cycles, these pollutions will accumulate in the recycled paper, resulting in lower paper quality [15–17].

A highly hydrophilic barrier layer is preferred against oxygen, for example, coatings based on cellulose or starch [18–21]. The disadvantage of using these materials is, however, that the oxygen barrier performance is sensitive to high humidity. Water acts as a plasticizer when it is absorbed by the polymer coating, which increases the intermolecular distance of the polymer chains. This causes an increase in the mobility of the polymer chains and a concomitant higher diffusion rate of gases through the coating which reduces its barrier performance [20,22,23]. Hydrophobic coatings, such as waterborne coatings based on polystyrene and/or polyacrylates, have the benefit of imparting water resistance and reducing humidity sensitivity [24–27]. Optimal gas barrier coatings for both oxygen and water vapor can be obtained when the hydrophobicity and hydrophilicity of such coatings are well balanced [18,28,29]. A commonly used paper-based food packaging that has excellent barrier performance against multiple migrants is a composite consisting of paper, polyethylene, and aluminum. Separating and recycling the individual layers is, however, very challenging and only possible with extensive chemical treatments [30,31]. A water-soluble release layer between the barrier coating and paperboard can be helpful to easily separate the coating from the paperboard so that it does not hinder recyclability of the paperboard; for example, a polyvinyl alcohol coating on paperboard [32].

Alkali-soluble resin-stabilized (ASR) waterborne coatings are interesting as liquid water and oil barrier coatings on paperboard, as shown in our previous work [33,34]. This ASR consists of both hydrophilic and hydrophobic moieties, acrylic acid, and styrene , which are favorable for potential gas barrier performance against both oxygen and water vapor. An ASR-stabilized polymer dispersion was synthesized using emulsion copolymerization of styrene and *n*-butyl acrylate in presence of an alkaline aqueous ASR solution [35]. The resulting dispersion was conveniently applied on untreated paperboard by bar-coating, and during drying both water and base evaporate, causing the protonation of the carboxylic acids in the ASR, resulting in a water-insoluble coating [36–40]. The barrier penetration mechanism of these waterborne coatings is different for liquid water and oils: water is absorbed by the coating and the water barrier properties are influenced by the carboxylate concentrations in the coating, while oil penetrates via the defects in the coating [33]. These ASR-stabilized waterborne coatings can in principle be removed from the substrate by immersion in alkaline aqueous solution since that leads to deprotonation of the carboxylic acids in the ASR and subsequent dissolution in the alkaline water phase [41]. However, the gas barrier properties and recyclability of ASR-stabilized waterborne coatings have been rarely studied.

Herein, the gas barrier performance of ASR-stabilized waterborne coatings on paperboard for N_2, CO_2, O_2, and H_2O vapor is investigated. Insight is given into the different permeation mechanisms for the various gasses. Also, preliminary results attempting to remove the ASR-stabilized waterborne coating from paperboard are reported.

2. Experimental Section

2.1. Materials

The monomers styrene (S, ≥99%) and *n*-butyl acrylate (BA, ≥99%) were purchased from Sigma Aldrich, Amsterdam, The Netherlands, and both were used as supplied. The thermal initiator, ammonium persulfate, and the dissolved alkali-soluble resin (ASR) were used as received from BASF, Heerenveen, The Netherlands. Details about the ASR were previously described [34]. Isopropanol (IPA, ≥99.5%) was purchased from Sigma-Aldrich. Sodium hydroxide (NaOH, 98.5%) salt is obtained from Acros Organics, Geel, Belgium. All chemicals were used as supplied. Demineralized water was used throughout this research. The paperboard substrate was kindly provided by Storaenso, Amsterdam, The Netherlands, type 'Ensocard'. This is an uncoated bleached board having a thickness of 215 μm (170 g/m^2).

2.2. Coating Prepration

The polymer dispersion of styrene and *n*-butyl acrylate stabilized by the ASR was prepared via a semi-batch emulsion polymerization, and described in detail in our previous work [34]. For the coatings used in the gas barrier measurement, the as-prepared dispersion was added to the isopropanol (IPA, 5 wt%) and mixed by hand. Subsequently, the coatings were prepared by applying ca. 1.5 mL of the polymer dispersion on a paperboard substrate (18 × 30 cm) and making a 'draw-down' using a bar-coater (RK control coaster, speed level 8, 12 or 24 μm wet deposit wire bar). The coatings were dried at 60 °C for 1 h in a ventilated oven. This process was repeated for the double and triple coating layers, i.e., the next layer was applied after drying the previous layer at 60 °C for 1 h. After drying, the coatings were stored under ambient conditions for further characterization.

2.3. Coating Characterization

Scanning electron microscopy (SEM) images were taken off the surface and cross-section of the coatings applied on paperboard. The cross-section was prepared by cryogenic breaking of the sample in liquid nitrogen. All samples were covered with a conducting layer by sputter coating with gold (30 s at 30 mA), and images were taken with SEM (JEOL 7800F, Nieuw-Vennep, The Netherlands) in secondary electron mode. The thickness of the coating layer was estimated by analyzing the cross-sections of the samples in the SEM images.

Attenuated total reflection Fourier-transform infrared spectroscopy (ATR-FTIR, Varian-Cary, Varian 670 IR equipped with a golden gate setup and Ge crystal, Vlissingen, The Netherlands) was measured from the samples. For easy comparison, the spectra were corrected with a simple baseline correction and normalized at the vibration peak at 2930 cm^{-1} using the program SpectraGryph 1.2.

The particle size was determined by dynamic light scattering (DLS, Zetasizer Nano Series, Malvern Instruments, Eindhoven, The Netherlands) to obtain the particle diameter. Dispersions were diluted with demineralized water or 0.1 M NaOH solution and filtered (GE healthcare, glass microfiber filter with polypropylene housing, pore size of 2 μm) before measuring.

2.4. Single Gas Barrier Performance

Gas permeation measurements of the single gasses He, N_2 and CO_2 were performed in a stainless-steel cell with an area of 2.1 cm^2. The coated paperboard samples were placed in the cell and equilibrated overnight under He feed pressure of 2 bar and vacuum at the permeate side. All samples were measured at 20 °C. The permeate pressure increase was measured over time for each gas. Using the ideal gas law in Equation (1), where Δn [mol] is the amount of gas, ΔP [Pa] is the increase in permeate pressure, V_c [m^3] is calibrated permeate volume, R [J/K·mol] is the gas constant and T [K] permeate temperature, and molar volume V_m [cm^3/mol], the permeate volume $V_{permeate}$ [cm^3] was calculated (Equation (2)).

The permeability was determined using Equation (3), where P_i [$cm^3/(m^2 day)$], A [m^2] is the measured area, and t [day] is the time.

$$\Delta n = \frac{\Delta P \times V_c}{R \times T} \quad (1)$$

$$V_{permeate} = \frac{\Delta n}{V_m} \quad (2)$$

$$P_i \left[\frac{cm^3}{m^2 \times day}\right] = \frac{V_{permeate}}{A \times t} \quad (3)$$

2.5. Water Vapor Transmission Rate (WVTR)

A cup was filled with dry silica gel (orange color) up to ca. 0.5 cm under the edge of the cup. The coatings were cut to round samples with an area of 29.2 cm^2 and were then placed on top of the cup with the coated side facing the silica. The sample was sealed by closing the lid and placed in a climate chamber of 85% RH and 23 °C for seven days. The WVTR-values were determined gravimetrically and expressed in [$g/(m^2 \cdot day)$]. The liquid water barrier performance was using the gravimetrical Cobb method, which was described previously [34].

2.6. Oxygen Transmission Rate (OTR)

The coating substrates were cut to round samples having an area of 100 cm^2 and were placed on top of the permeation cell (V = 100 cm^3) with the coated side facing inwards. The edges of the cell were greased to ensure airtight closure. The inside of the cell was flushed with nitrogen to remove all oxygen. The sample was then exposed to environmental air for 24 h, and the oxygen concentration inside the cell was monitored over time. The data were converted to a dynamic accumulation plot of which the slope was multiplied by the cell volume and subsequently divided by the substrate surface to give the OTR [$mL/(m^2 \cdot day)$].

2.7. Coating Removal

The coating applied on paperboard was removed by adding 0.1 M NaOH (aq) solution on top of the paperboard after 5 min, after which the paperboard was rinsed with demineralized water. For immersion, coated paperboard was immersed for 5 min in 0.1 M NaOH solution followed by rinsing with demineralized water. In both cases, the paperboard was dried under vacuum overnight before characterization.

3. Results and Discussion

3.1. Gas Barrier Performance

3.1.1. Characterization of the Waterborne Coating on Paperboard

The ASR-stabilized dispersion was prepared by emulsion polymerization of styrene and *n*-butyl acrylate monomers and thermally initiated with ammonium persulfate as previously reported [34]. Our previous work showed that addition of 5 wt% isopropanol (IPA) to the polymer dispersion was beneficial for the oil barrier performance of the applied coating on paperboard as it improved the spreading of the dispersion on the paperboard and reduced the number of defects in the coating [33]. The dispersion with 5 wt% IPA was applied on the untreated paperboard by bar-coating and dried at 60 °C for 1 h. The second and third coating layers were applied via the same method taking an hour of drying time in-between layers into account (Figure 1A,B). The gas barrier performance was evaluated for coatings consisting of one, two, or three coating layers.

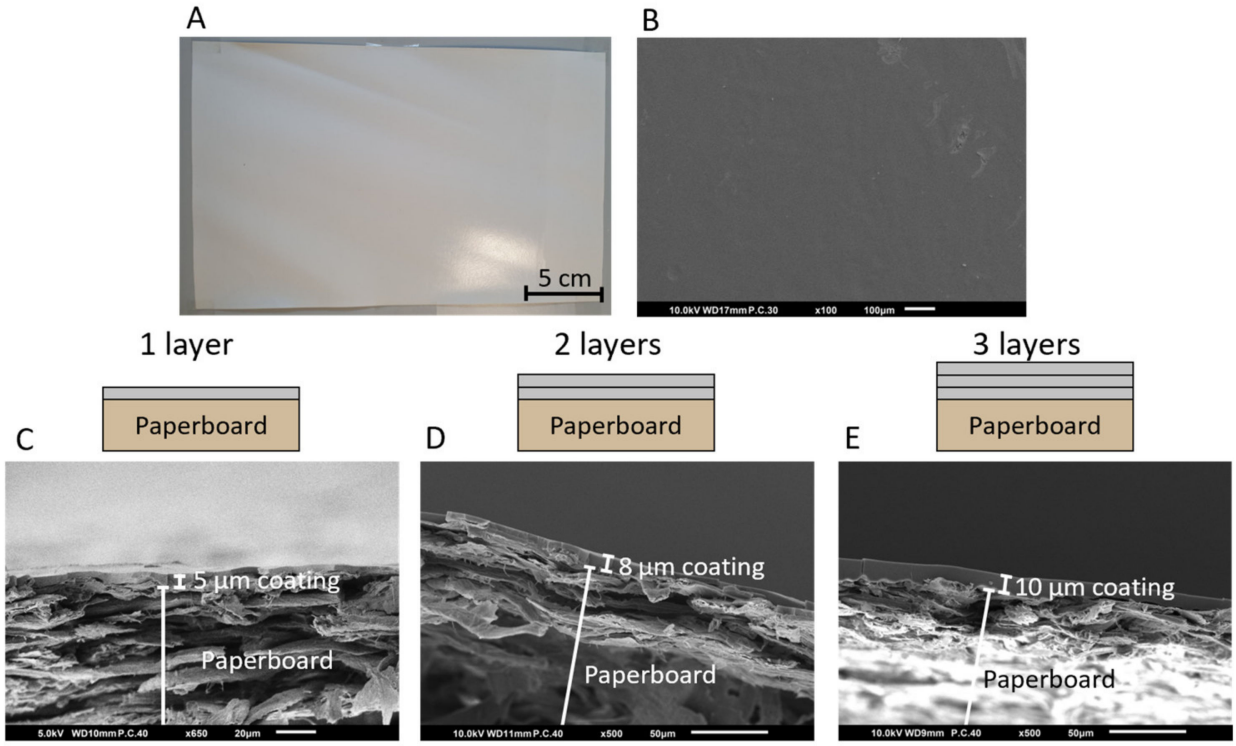

Figure 1. (**A**) SEM image and (**B**) photograph of the surface of the triple-layer coating on paperboard. SEM images of the cross-section of coated paperboard with corresponding coating thickness of (**C**) one, (**D**) two and (**E**) three coating layers. The waterborne coatings are obtained by applying an ASR-stabilized dispersion containing 5 wt% isopropanol on paperboard.

The coatings on paperboard were further analyzed by scanning electron microscopy (SEM). The thickness of the coatings was determined from the SEM images in Figure 1. The coatings formed a continuous and smooth layer on top of the porous and fibrous structure of the untreated paperboard. The thickness of a single-layer coating was 5 µm (Figure 1C), and applying a second layer on top increased the thickness to 8 µm (Figure 1D). The thickness increase of the third coating layer was less compared to the double-layer coating, giving an overall final thickness of 10 µm (Figure 1E). The first coating layer was applied on untreated, porous and rough paperboard. Likely, more material was applied by bar-coating to fill the pores of the paperboard compared to the second and third coating layers. Possibly, another effect also plays a role in the varying thicknesses for the first and following coating layers. During application of the first coating layer, water is immediately absorbed by the paperboard, causing a slight increase in the dry solid content. For the second and third coating layers, the first coating layer hinders water absorption by the paperboard, therefore, less polymer material was deposited for the second or third coating layers.

3.1.2. Oxygen and Water Vapor Barrier Properties

The effect of the number of coating layers on the gas barrier performance was first evaluated by measuring the permeation of oxygen and water vapor. The oxygen transmission rate (OTR) was determined by measuring the oxygen concentration increase inside a nitrogen-filled cell sealed by the coated paperboard when exposed to air. Air is a mixture of N_2 (78.08%), O_2 (20.95%), Argon (0.9%), CO_2 (0.04%) and other small traces of gases [42]. Importantly, the air had a relative humidity (RH) of 50% to 60%, thus water vapor also is present in air. The OTR of a single-layer coating, shown in Figure 2A was very high (6.2×10^4 $cm^3/(m^2 \cdot day)$), and applying a second coating layer reduced the OTR by a factor of 3 to 2.3×10^4 $cm^3/(m^2 \cdot day)$. Applying the second coating layer reduced the number of coating defects, which is beneficial for lowering gas permeation. The oxygen barrier was

significantly improved by applying a third coating layer, as evidenced by a twenty-fivefold decrease of the OTR value to 9.2 × 10^2 $cm^3/(m^2 \cdot day)$ compared to double-layer coatings. This large improvement in barrier performance is remarkable, since with applying the third coating layer, only 2 extra µm is added to the total thickness. This third coating layer was applied on an even smoother surface than the second layer, and during drying the overall polymer coating was exposed to 60 °C for two additional hours which, might have improved the barrier performance [43–46]. Reference values for maximum accepted permeabilities are challenging to find and depend on the type of packed food. A value found in literature is that the OTR should be lower than 15 $cm^3/(m^2 \cdot day)$ to become interesting for the food packaging application [47], however, it should be highlighted that a direct comparison is not possible due to differences in layer thickness. In fact, the large majority of the literature reported OTR values do not specify the thickness of the layers used to determine those values, which, in our view, should be reported. Hence, we report the thickness of our coating layers but to avoid confusion, do not include it in the OTR and WVTR calculated values.

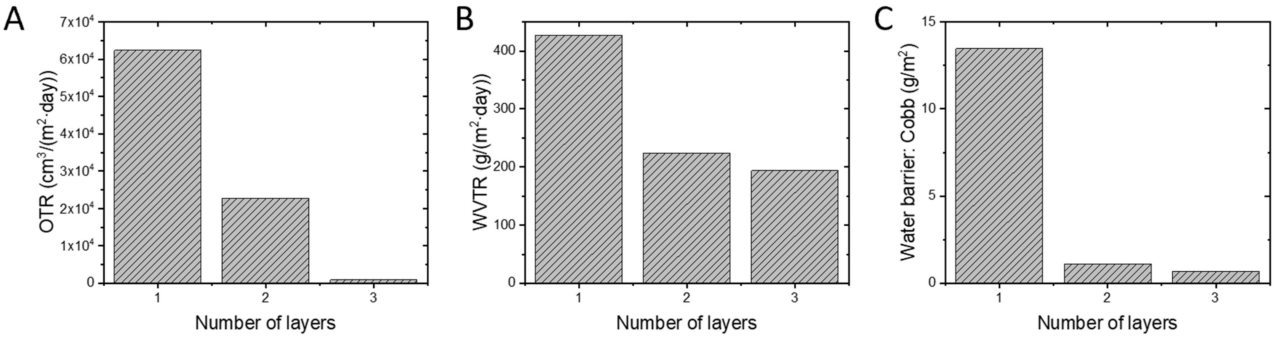

Figure 2. Barrier performance of (**A**) oxygen (OTR), (**B**) water vapor (WVTR) and (**C**) liquid water (Cobb) of coated paperboard with one, two or three coating layers.

Both the barrier performances against water vapor and liquid water were also determined (Figure 2B,C). Both vapor and gas are in the gas phase, but for a vapor, the species can also occur as a liquid or solid at a specific temperature, while a gas can only exist as such at the specific temperature. The water vapor transmission rate (WVTR) was determined by sealing a cup filled with anhydrous silica with the coated paperboard. The cup is exposed to 23 °C and 85% RH. The mass increase by water absorption of the silica is measured over time. The single layer coating showed a WVTR of 430 $g/(m^2 \cdot day)$ and this value was almost halved to 240 $g/(m^2 \cdot day)$ for the double-layer coating. Applying a third coating layer gave a value of 200 $g/(m^2 \cdot day)$. Also, for the WVTR applies that comparing our value to a reference value is challenging due to differences in thickness of the tested layers. In addition, the substate can also have a huge impact. According to the literature, the WVTR should be lower than 10 $g/(m^2 \cdot day)$ to be considered as a high barrier coating for food packaging [47]. The water vapor barrier improvement by applying more layers is less pronounced compared with the oxygen barrier results. Most likely, this effect can be explained by the difference in barrier mechanism. From our previous work, it is known that the amount of water vapor absorbed by the coating is RH dependent [34]. The higher the RH, the more water is absorbed by the coating. Since applying the third coating layer did not improve the water vapor barrier performance significantly, this is an indication that the water vapor barrier is less dependent on the number of defects in the coating.

The liquid water barrier performance (Figure 2C) was measured using the gravimetrical Cobb method, i.e., the difference in mass before and after 10 min of water exposure. Cobb value of 13.5 g/m^2 for single-coated paperboard was found. This value was decreased enormously to 1.1 g/m^2 by applying a second coating layer. A smaller improvement was observed when the third coating layer was applied (0.7 g/m^2) compared to double-layer coatings. The strong improvement in water barrier performance when applying the second

coating layer is explained by filling and covering the large surface defects present in the first coating layer with the second coating layer. There are hardly any large defects present in the second coating layer. Additionally, the barrier performance for liquid water is dependent on coating thickness as thicker coatings slow down the diffusion.

3.1.3. Carbon Dioxide and Nitrogen Barrier Properties

Apart from looking at the above-discussed barrier properties against oxygen and water (vapor), also barrier performance towards helium (He), N_2, and CO_2 was investigated. N_2 and CO_2 are interesting for modified atmosphere packaging, and He is measured as a reference. The effect of the number of coating layers on the gas barrier performance was first evaluated by measuring the permeation of anhydrous pure He, CO_2 and N_2 gases. For safety reasons, it was not possible to measure pure oxygen permeation in the same way as the other gases. The permeation of He, CO_2, and N_2 was measured using a stainless-steel cell having a pressure of two bars of the pure gas at the feed side and vacuum at the permeate side. This is the lowest pressure difference possible to measure with the used setup. However, in food packaging, the permeation is usually concentration driven and not pressure driven, except for vacuum-packed food. The gas permeation of He, CO_2, and N_2 for barrier coatings is rarely reported in literature, but the used measuring method has been reported for liquid crystalline polymer films [48].

The gas permeation of He, CO_2, and N_2 in Figure 3A showed two trends; first the permeation for all three gases decreased with increasing number of coating layers, and second for all samples, helium had the highest permeation compared to CO_2 and N_2. The single-layer coating has high permeabilities for He (2.7×10^7 $cm^3/(m^2 \cdot day)$), CO_2 (1.2×10^7 $cm^3/(m^2 \cdot day)$), and N_2 (1.5×10^7 $cm^3/(m^2 \cdot day)$). Applying a second coating layer lowers the permeation with a factor of approximately 3 for all three gases to permeabilities of 1.0×10^7 $cm^3/(m^2 \cdot day)$ for He, 4.2×10^6 $cm^3/(m^2 \cdot day)$ for CO_2 and 4.0×10^6 $cm^3/(m^2 \cdot day)$ for N_2. Surprisingly, applying a third coating layer dramatically decreased the permeation for all gasses with an additional factor of 100 to permeabilities of 7.6×10^4 $cm^3/(m^2 \cdot day)$ for He, 4.3×10^4 $cm^3/(m^2 \cdot day)$ for CO_2 and 3.9×10^4 $cm^3/(m^2 \cdot day)$ for N_2 (Figure 3B) compared to the double-layer coatings. A similar trend was found for the oxygen permeation (vide supra).

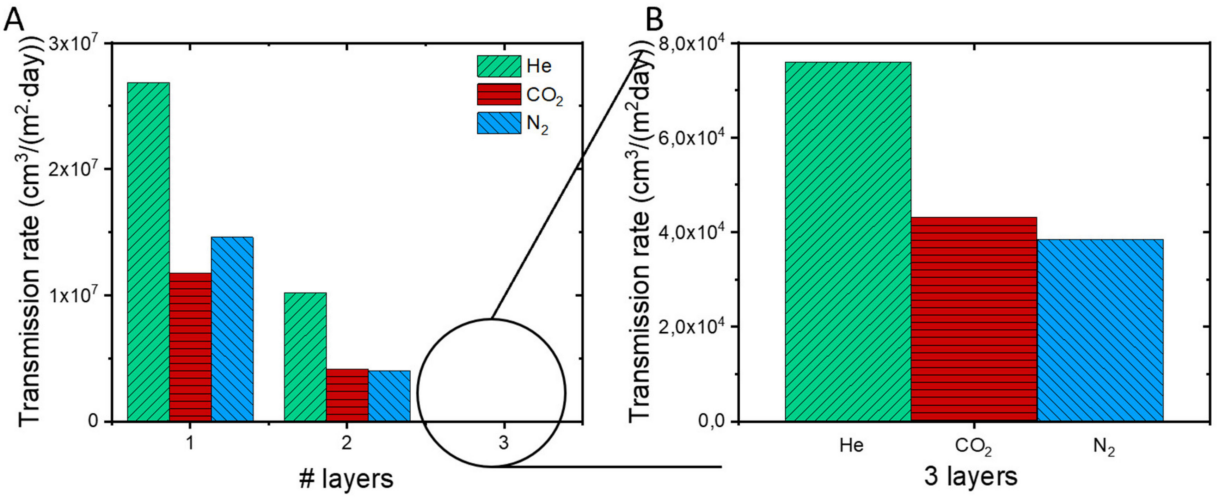

Figure 3. (**A**) Single gas permeability (He, CO_2 and N_2) of ASR-stabilized waterborne coatings on paperboard having one, two or three coating layers. (**B**) Zoom in on the triple-coated paperboard.

Helium has the highest permeation through the polymer coatings independent of the number of layers compared to CO_2 and N_2. The permeability (P) of dense coatings depends on the diffusion (D) and solubility (S) of the gas species as described in Equation (4) [49].

$$P = D \times S \quad (4)$$

The diffusion and solubility depend on the kinetic diameter and the critical temperature of the gas species, respectively [50]. The kinetic diameter is a measure of the diameter of the gas, which depends on mean free path and number of molecules per unit volume [49]. Helium has the smallest kinetic diameter, followed by CO_2 then N_2 (Table 1. Thus, based on the kinetic diameter, the diffusion is expected to be the highest for He, followed by CO_2 then N_2. The solubility of a gas into the polymer coating mainly depends on the condensability of a gas. The critical temperature of a gas is directly related to the condensability of a gas in a material and usually increases with increasing temperature, resulting in an increased solubility of the gas species in the polymer coating [51]. Helium has the lowest critical temperature, followed by N_2 then CO_2 (Table 1), indicating that helium has the lowest solubility, followed by N_2 then CO_2. However, it should be noted that not only the critical temperature but also the chemical affinity between gas and polymer matrix will influence the solubility.

Table 1. Kinetic diameter and critical temperature of the various investigated gases. Data retrieved from ref. [49].

Gas	Kinetic Diameter (nm)	Critical Temperature (°C)
He	0.26	−268
CO_2	0.33	31
O_2	0.35	−119
N_2	0.36	−147

Helium has the highest permeability for all coatings with one, two, or three coating layers because helium has the smallest kinetic diameter, resulting in the highest diffusion through the dense polymer coating. The permeation of N_2 and CO_2 are comparable for the coatings with two or three coating layers, which indicates that the difference between diffusion and solubility does not play a dominant role in the permeability of N_2 or CO_2 through the polymer coating. The permeability of O_2 should be similar to CO_2 and N_2 as the diffusion and solubility of O_2 are comparable with CO_2 and N_2. The diffusion depends on the kinetic diameter and the kinetic diameter of O_2 has a value between the kinetic diameters of CO_2 and N_2. The solubility depends on the critical temperature and the critical temperature of O_2 is slightly lower than N_2 (Table 1). However, the previously discussed OTR values were forty times lower compared with the permeation of He, CO_2, and N_2 for the three-layer coatings. This difference might be attributed to the use of a different setup for the OTR-measurement, where the concentration difference was the driving force for the permeation.

3.2. Recyclability of Coated Paperboard

3.2.1. Influence of Individual Base Treatments on Paperboard and Coating Material

From a sustainability point of view, paperboard food packaging should be recyclable. Therefore, it was explored whether the ASR-stabilized waterborne barrier coating can be conveniently removed from the paperboard. The single-layer waterborne coatings were formed by applying the ASR-based polymer dispersion on paperboard by bar-coating and drying in a ventilated oven at 60 °C for 1 h. During drying, water and volatile base (ammonia) are evaporated, resulting in the protonation of the carboxylates in the ASR to form the carboxylic acids. The hypothesis is that the coating can be removed from the paperboard by treating the coating with 0.1 M NaOH (aq) (pH = 13) (Figure 4A). During

this base treatment, it is expected that the carboxylic acids of the ASR deprotonate, resulting in a water dispersible coating while the paperboard itself remains unaffected (Figure 4B).

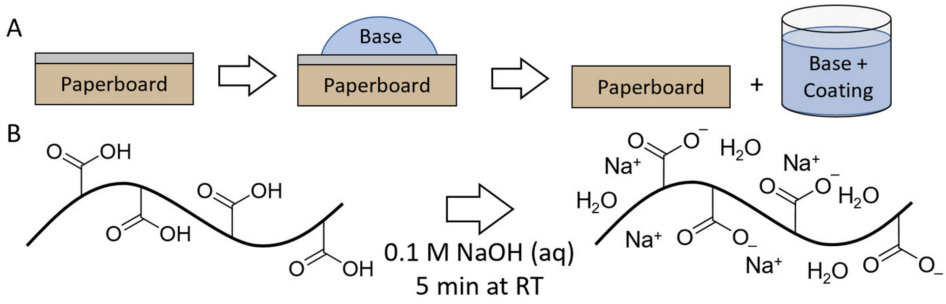

Figure 4. (**A**) Schematic representation of the base treatment of the waterborne coating. (**B**) Schematic depiction of the influence of base (0.1 M NaOH) on the carboxylic acids of the ASR causing deprotonation.

First, it was investigated how the two components of the system, the paperboard and coating material, were individually affected by the base treatment. The uncoated paperboard substrate was tested by depositing a drop of 0.1 M NaOH (aq) on top of the surface. After 5 min, the base was removed by extensively rinsing the paperboard with water and subsequently drying it in vacuum overnight before characterization. The paperboard was not affected by the base treatment, as Figure 5A–C shows identical SEM images and overlapping FTIR spectra of virgin and base-treated paperboard. The SEM images both show the fibrous structure of the surface of the paperboard. The FTIR spectra show several characteristic vibration peaks, namely at 3320 cm^{-1} (OH stretching), 2890 cm^{-1} (CH stretching), 1635 cm^{-1} (OH bending of absorbed water), and 1430–900 cm^{-1} (primarily, C-C stretching and COH and CCH deformation) [52,53].

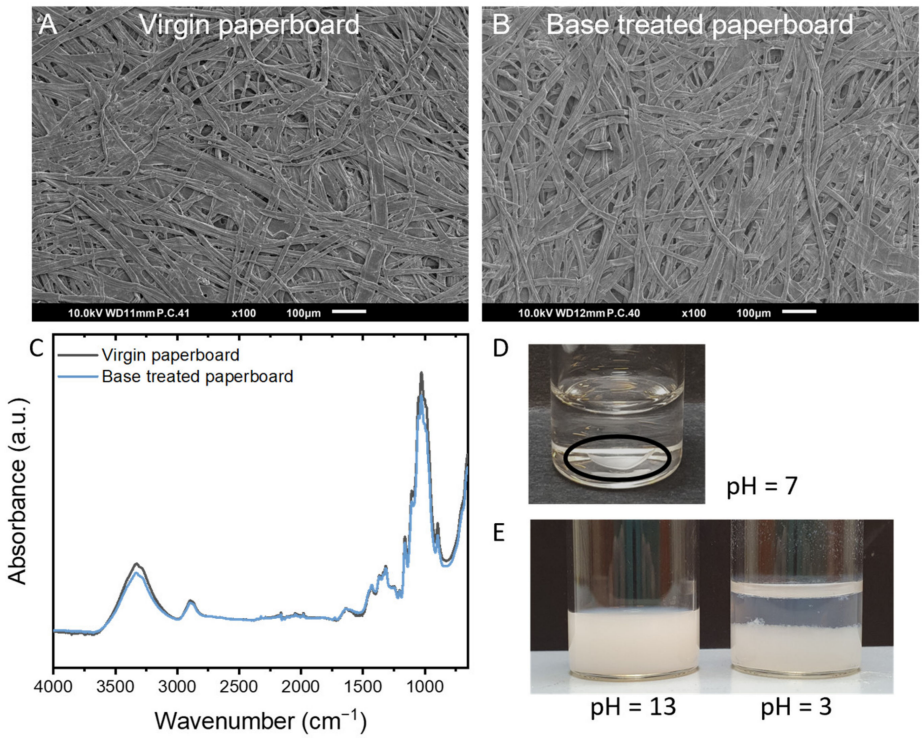

Figure 5. SEM images of the (**A**) virgin and (**B**) base-treated (0.1 M NaOH (aq) for 5 min) uncoated paperboard with (**C**) corresponding FTIR spectra. (**D**) Photograph of free-standing film (in black circle) immersed in demineralized water (pH = 7). (**E**) Photograph of free-standing film of the coating dispersed in pH = 13, followed by lowering the pH to 3 causing sedimentation of the polymers.

Next, a free-standing film of the dried ASR-stabilized dispersion was treated with a 0.1 M NaOH solution (pH = 13) to test if the ASR-stabilized waterborne coating could be re-dispersed in the alkaline solution; the treatment resulted in a homogenous milky liquid (Figure 5E), indicating that the alkaline solution can potentially be used for removing the coating from the paperboard (vide infra). As a reference, the free-standing film was immersed in demineralized water (pH = 7) which showed that under neutral condition, the film remained intact and became white (Figure 5D). This data shows that the paperboard is unaffected upon contact with alkaline water, and that the waterborne coating re-disperses in alkaline water during the base treatment.

Interestingly, lowering the pH to acidic conditions (pH = 3) causes the polymer phase to sediment as shown in Figure 5E. In this acidic environment, the carboxylates of the ASR protonate to carboxylic acids which are no longer able to electrostatically stabilize the poly (styrene/butyl acrylate) particles as the ASR becomes water-insoluble. This results in an unstable polymer dispersion where the polymers precipitate under acidic conditions. This precipitate can subsequently be separated from the aqueous phase by filtration.

3.2.2. Influence of Base Treatment of Coated Paperboard

Having determined the effect of the base on the individual components, the next step was to investigate if a coating applied on paperboard can be removed upon 0.1 M NaOH (aq) base treatment. The ASR-stabilized dispersion was applied on paperboard by bar-coating and dried at 60 °C for 1 h. The porous and fibrous surface of the paperboard was effectively covered with waterborne coating as shown by the SEM image in Figure 6A. A droplet of 0.1 M NaOH (aq) was then placed on top of the coated paperboard for 5 min, followed by an extensive rinsing step with demineralized water. The treated paperboard was dried under vacuum overnight before further characterization. Then the surface was analyzed using SEM and FTIR (Figure 6B,C). The SEM image shows the fibrous structure of the paperboard; however, some residues of the coating were observed when compared to the surface of virgin paperboard. The corresponding FTIR spectra show that after base treatment the surface of the treated paperboard strongly overlaps with the untreated paperboard with almost no trace of the coating. The vibration peaks at 1730 and 700 cm^{-1} differ from the spectrum of pure paperboard and correspond to the C=O stretching vibration of the *n*-butyl acrylate and the mono-substituted aromatic group in styrene of the poly(styrene/butyl acrylate) core, respectively. Thus, base treatment of coated paperboard removed the ASR-stabilized single-layer waterborne coating to a large extent, while traces of the poly(styrene/butylacrylate core remained.

3.2.3. Re-Using Paperboard

After the above discussed initial studies on individual components and dropwise application of the NaOH solution, the base treatment was changed to a more industrial relevant process. Rather than placing a drop of alkaline solution on top of the coating, the coated paperboard was immersed in 0.1 M NaOH solution for 5 min to remove the waterborne coating from paperboard (Figure 7A). During the immersion step, the base is also absorbed by the paperboard. Thus, the base penetrates from two sides, via the coating/air and coating/paperboard interfaces. After immersion, the treated paperboard was rinsed with water, and the treated samples were dried under vacuum before characterization. After drying, the treated paperboard was deformed (Figure 7B). In Figure 7C the SEM image shows less coating residues on the fibrous surface of the immersed paperboard than paperboard treated with a single droplet.

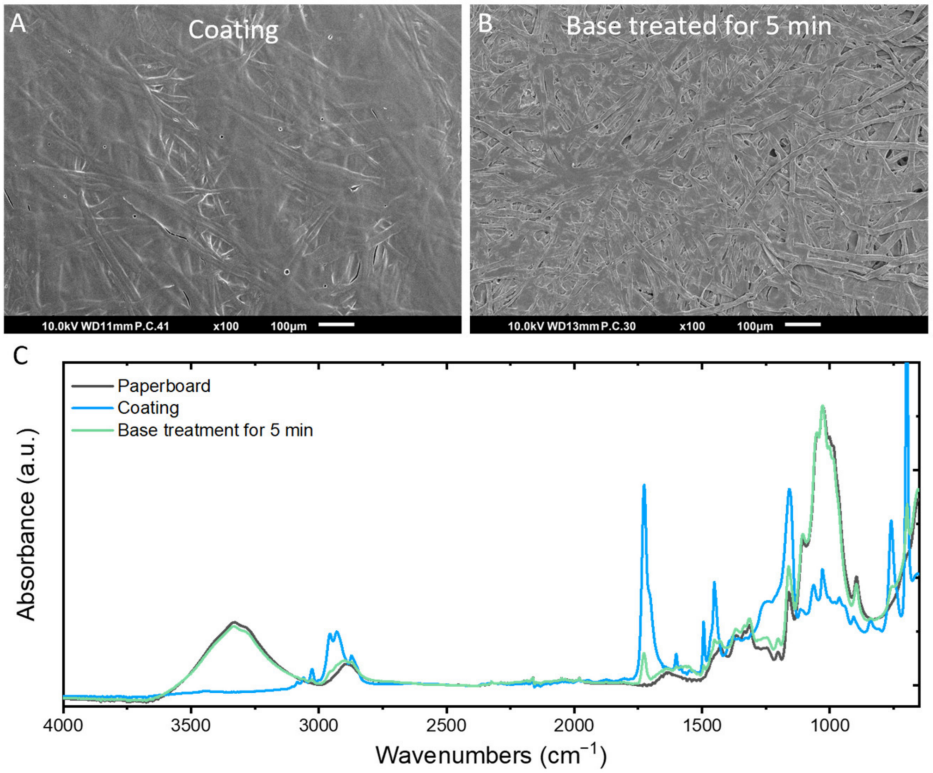

Figure 6. SEM images of the (**A**) initial coating on paperboard and (**B**) base-treated coating (0.1 M NaOH (aq) for 5 min) on paperboard. (**C**) Corresponding FTIR spectra of paperboard, coating and base-treated coating.

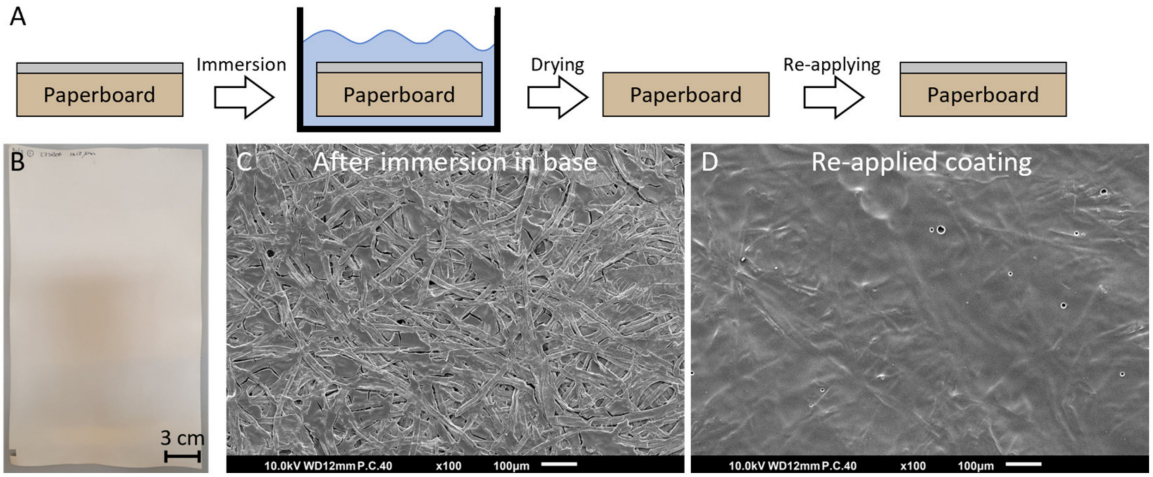

Figure 7. (**A**) Schematic representation of the base treatment by immersing the coated paperboard in 0.1 M NaOH for 5 min and subsequently extensive rinsing with demineralized water. After drying the treated paperboard under vacuum overnight, a new coating layer was re-applied on the paperboard. (**B**) Photograph and (**C**) SEM image of the coated paperboard was immersed in 0.1 M NaOH solution for 5 min and dried in vacuum overnight. Subsequently, (**D**) SEM image after applying a new coating layer on the base-treated paperboard.

To investigate if the 'recycled, cleaned' paperboard could be re-used as a substrate for subsequent barrier coatings, a new coating layer was applied by bar-coating. This new coating layer covered the paper fibers, but surface defects were observed (Figure 7D). These surface defects are also present in the initially coated paperboard, which are formed during drying as described in our previous work [33]. The water barrier performance of the

coating was then re-determined by the gravimetrical Cobb method. A value of 13.5 g/m^2 was measured for the initially applied coating on paperboard and after coating removal and re-application, a value of 330 g/m^2 was found. The water barrier performance decreased enormously, which might be caused by the deformation and curling of the treated and dried paperboard compared to virgin paperboard. Probably, the coating is also too thin to form a sufficient water barrier.

3.2.4. Multilayer Barrier Coatings

In Section 2.1, we described that the best gas barrier properties were obtained for multilayer coatings. Therefore, the effect of the base treatment on a double-layer coating was also investigated. When a droplet of 0.1 M NaOH solution was placed on top of the double-coated paperboard, after 30 s the surface was affected by the base as can be seen in Figure 8A. After 5 min of base treatment, cracks were observed in the coating layer and some of the paper fibers were visible in the SEM images (Figure 8B). The FTIR spectra in Figure 8D show that after 30 s of base treatment, the coating vibration peaks were more intense than the paperboard vibration peaks. Increasing the base treatment time to 5 min, the paperboard vibration peaks became stronger compared to the coating vibration peaks. This indicates that with increasing base-treatment time, more coating was removed from the paperboard.

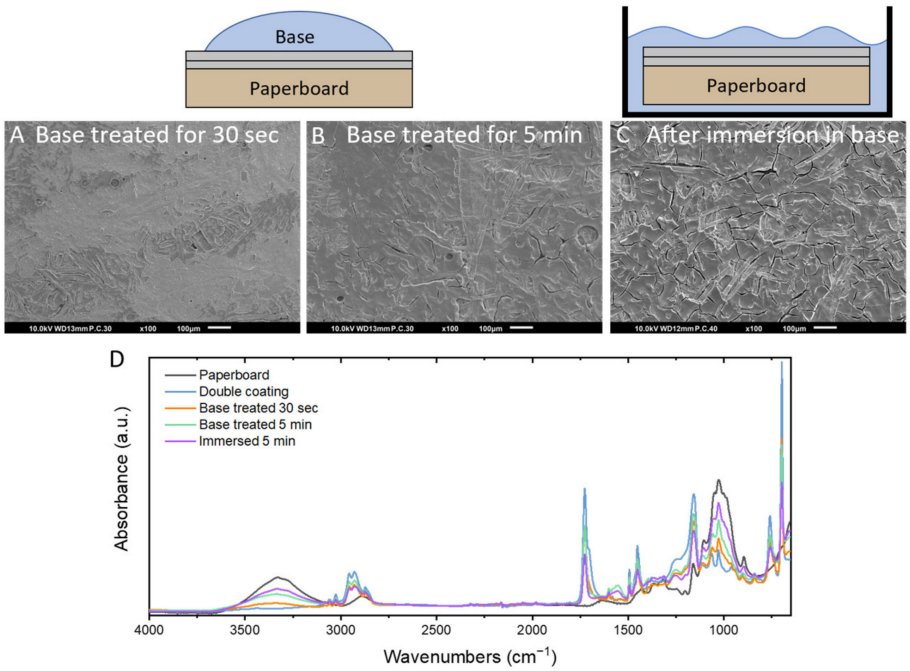

Figure 8. SEM images of the base-treated double-coated paperboard by placing a droplet of 0.1 M NaOH (aq) on top for (**A**) 30 s and (**B**) 5 min. Additionally, (**C**) the double-coated paperboard was immersed in 0.1 M NaOH solution for 5 min. (**D**) Corresponding FTIR spectra of the uncoated, double-coated paperboard and base-treated coating.

It was more difficult to remove the double layer coating from the paperboard than a single layer coating. The second coating layer dried differently compared to the first coating layer. During drying of the first coating layer, water is evaporated from the coating/air interface and water is absorbed by the paperboard. During drying of the second coating layer, water can only evaporate via the air/coating interface as the first coating layer hinders the water uptake by the paperboard. Additionally, the double layer coating has an interface between the two coating layers, and it could be that due to this coating/coating interface, removal of the coating by the drop method is hindered by the poor penetration of the droplet into the double-layer coating.

In contrast, when a double coated paperboard is immersed in a 0.1 M NaOH (aq) solution for 5 min, the alkaline solution can affect the coating from both air/coating and paperboard/coating interfaces as the base is absorbed by the paperboard. The SEM image in Figure 8C shows a combination of small coating residues and paper fibers. Based on the SEM image and FTIR spectra, it appears that immersion was more effective in removing the coating from the paperboard than only applying the base to the top of the coating.

To investigate why the double layer coatings are more challenging to remove, also a thick single layer coating was applied on paperboard and treated with 0.1 M NaOH solution. When the alkaline droplet was placed on top of the thick single layer coating, after 30 s small cracks were formed in the coating surface (Figure 9A). After 5 min, the fibers were visible with minor coatings residue over a large fraction of the surface (Figure 9B). Upon immersion of the thick single-coated paperboard in alkaline solution, almost all the polymer coating was removed from the paperboard (Figure 9C). These results indicate that 5 min of base treatment was sufficient to remove a thick single coating layer from the paperboard. When a double layer is applied, 5 min is insufficient to remove the coating. These results clearly indicate that the difference between the double coatings and single thick coating, the additional interface between the two coating layers for the double coatings, can be the reason for the lower efficiency in removing the double layer coating, as it hinders or slows down the base penetration throughout the polymer layer towards the substrate interface.

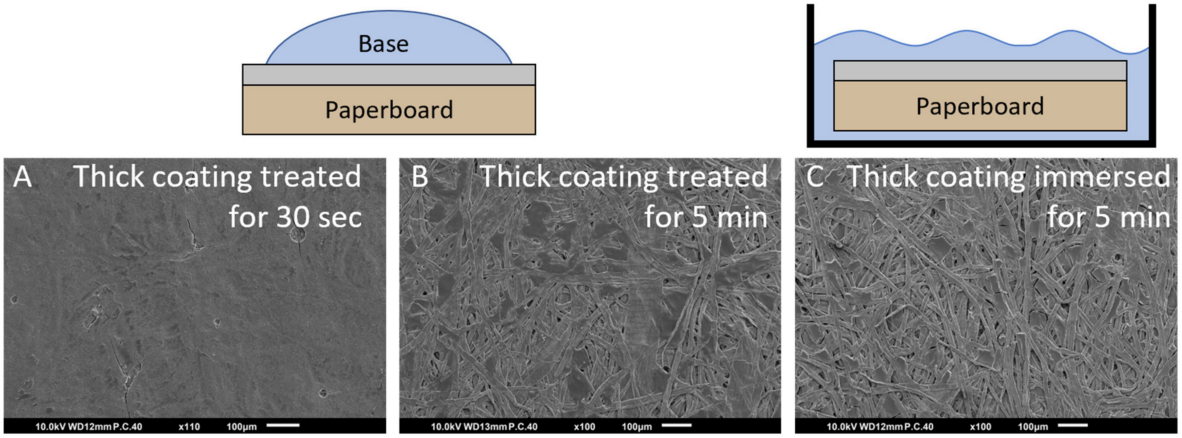

Figure 9. SEM images of the single thick coating on paperboard treated with 0.1 M NaOH (aq) by placing a droplet on top of the coated paperboard for (**A**) 30 s and (**B**) 5 min. Additionally, (**C**) the single thick coated paperboard was immersed in 0.1 M NaOH solution for 5 min.

4. Conclusions

ASR-stabilized waterborne coatings with varying number of coating layers were applied on paperboard by bar coating. Barrier properties of these ASR-stabilized waterborne coating are dependent on relative humidity, since absorbed water acts as a plasticizer and leads to decreased barrier performance [20,22]. The permeation of CO_2, N_2, and O_2 decreased with an increasing number of coating layers. Applying a second coating layer covers the surface defects of the first coating layer, thereby improving the barrier performance. Surprisingly, applying a third coating layer dramatically reduced the permeability even though the coating thickness only increased by 2 µm. Water vapor has a different permeation mechanism compared to the permeation mechanism of the other investigated gases because water is absorbed by the polymer coating. The water vapor barrier performance showed the largest improvement when a second coating layer was applied because this layer reduces the defects of the first layer, and increased the thickness significantly.

Interestingly, the ASR-stabilized waterborne coating can be removed from the paperboard substrate under alkaline aqueous conditions at room temperature. During base treatment, the carboxylic acids in the ASR deprotonate which results in dissolution of the ASR. As a result of this conversion, the coating was able to re-disperse in alkaline water.

The re-dispersed polymers can subsequently be precipitated by lowering the pH of the solution to acidic conditions. The paperboard was not affected by the base treatment. The single layer coating was almost fully removed upon base treatment. Removing double layer coatings from the paperboard was more challenging.

Overall, our results will help to understand and improve gas barrier properties and recyclability of polymer-coated paperboard for more sustainable packaging applications.

Author Contributions: Conceptualization, S.B., G.A.M., A.C.C.E. and A.P.H.J.S.; methodology, S.B.; validation, S.B.; formal analysis, S.B. and J.K.; investigation, S.B. and J.K.; writing—original draft preparation, S.B.; writing—review and editing, S.B., J.K., G.A.M., A.C.C.E. and A.P.H.J.S.; visualization, S.B.; supervision, A.P.H.J.S., G.A.M. and A.C.C.E.; project administration, A.P.H.J.S.; funding acquisition, A.P.H.J.S. and G.A.M. All authors have read and agreed to the published version of the manuscript.

Funding: This work is part of the Advanced Research Center for Chemical Building Blocks (ARC CBBC, 2018.010.B) which is cofounded and cofinanced by The Netherlands Organization for Scientific Research (NWO) and The Netherlands Ministry of Economic Affairs.

Institutional Review Board Statement: Not applicable.

Informed Consent Statement: Not applicable.

Data Availability Statement: Not applicable.

Acknowledgments: The authors thank Michael Debije for proof-reading the manuscript.

Conflicts of Interest: The authors declare no conflict of interest.

References

1. Cichello, S.A. Oxygen Absorbers in Food Preservation: A Review. *J. Food Sci. Technol.* **2015**, *52*, 1889–1895. [CrossRef] [PubMed]
2. M Rangaraj, V.; Rambabu, K.; Banat, F.; Mittal, V. Natural Antioxidants-Based Edible Active Food Packaging: An Overview of Current Advancements. *Food Biosci.* **2021**, *43*, 101251. [CrossRef]
3. Pittia, P.; Sacchetti, G. Antiplasticization Effect of Water in Amorphous Foods. A Review. *Food Chem.* **2008**, *106*, 1417–1427. [CrossRef]
4. Embleni, A. Modified Atmosphere Packaging and Other Active Packaging Systems for Food, Beverages and Other Fast-Moving Consumer Goods. In *Trends in Packaging of Food, Beverages and Other Fast-Moving Consumer Goods (FMCG)*; Woodhead Publishing Limited: Philadelphia, PA USA, 2013; pp. 22–34, ISBN 9780857095039.
5. Mujtaba, M.; Lipponen, J.; Ojanen, M.; Puttonen, S.; Vaittinen, H. Trends and Challenges in the Development of Bio-Based Barrier Coating Materials for Paper/Cardboard Food Packaging; a Review. *Sci. Total Environ.* **2022**, *851*, 158328. [CrossRef] [PubMed]
6. Tiseo, I. Packaging Market in the Netherlands in 2020, by Type of Material. Available online: https://www.statista.com/statistics/712415/packaging-market-in-the-netherlands-by-type-of-material/ (accessed on 5 August 2022).
7. Tiseo, I. Containerboard Consumption Worldwide from 2020 to 2031. Available online: https://www.statista.com/statistics/1090439/global-containerboard-demand/ (accessed on 1 August 2022).
8. Tiseo, I. Market Size of Paperboard Packaging Worldwide in 2021 and 2026. Available online: https://www.statista.com/statistics/1030199/market-value-of-paper-worldwide/ (accessed on 5 August 2022).
9. Tyagi, P.; Samaher, K.; Hubbe, M.A.; Pal, L. Advances in Barrier Coatings and Film Technologies for Achieving Sustainable Packaging of Food Products–A Review. *Trends Food Sci. Technol.* **2021**, *115*, 461–485. [CrossRef]
10. Anukiruthika, T.; Sethupathy, P.; Wilson, A.; Kashampur, K.; Moses, J.A.; Anandharamakrishnan, C. Multilayer Packaging: Advances in Preparation Techniques and Emerging Food Applications. *Compr. Rev. Food Sci. Food Saf.* **2020**, *19*, 1156–1186. [CrossRef] [PubMed]
11. Tiseo, I. Recycling Rate of Paper and Cardboard Packaging Waste in the European Union from 2005 to 2019. Available online: https://www.statista.com/statistics/974705/recycling-rate-of-paper-and-cardboard-packaging-waste-in-the-eu/ (accessed on 6 September 2022).
12. Bajpai, P. Process Steps in Recycled Fibre Processing. In *Recycling and Deinking of Recovered Paper*; Elsevier: Waltham, MA, USA, 2014; pp. 55–83, ISBN 9780124169982.
13. Nazhad, M.M. Recycled Fiber Quality- A Review. *J. Ind. Eng. Chem.* **2005**, *11*, 314–329.
14. Han, N.; Zhang, J.; Hoang, M.; Gray, S.; Xie, Z. A Review of Process and Wastewater Reuse in the Recycled Paper Industry. *Environ. Technol. Innov.* **2021**, *24*, 101860. [CrossRef]
15. Pivnenko, K.; Eriksson, E.; Astrup, T.F. Waste Paper for Recycling: Overview and Identification of Potentially Critical Substances. *Waste Manag.* **2015**, *45*, 134–142. [CrossRef]

16. Geueke, B.; Groh, K.; Muncke, J. Food Packaging in the Circular Economy: Overview of Chemical Safety Aspects for Commonly Used Materials. *J. Clean. Prod.* **2018**, *193*, 491–505. [CrossRef]
17. Suciu, N.A.; Tiberto, F.; Vasileiadis, S.; Lamastra, L.; Trevisan, M. Recycled Paper-Paperboard for Food Contact Materials: Contaminants Suspected and Migration into Foods and Food Simulant. *Food Chem.* **2013**, *141*, 4146–4151. [CrossRef]
18. Koivula, H.M.; Jalkanen, L.; Saukkonen, E.; Ovaska, S.-S.; Lahti, J.; Christophliemk, H.; Mikkonen, K.S. Machine-Coated Starch-Based Dispersion Coatings Prevent Mineral Oil Migration from Paperboard. *Prog. Org. Coat.* **2016**, *99*, 173–181. [CrossRef]
19. Christophliemk, H.; Johansson, C.; Ullsten, H.; Järnström, L. Oxygen and Water Vapor Transmission Rates of Starch-Poly(Vinyl Alcohol) Barrier Coatings for Flexible Packaging Paper. *Prog. Org. Coat.* **2017**, *113*, 218–224. [CrossRef]
20. Tayeb, A.H.; Tajvidi, M.; Bousfield, D. Paper-Based Oil Barrier Packaging Using Lignin-Containing Cellulose Nanofibrils. *Molecules* **2020**, *25*, 1344. [CrossRef] [PubMed]
21. Türe, H.; Gällstedt, M.; Johansson, E.; Hedenqvist, M.S. Wheat-Gluten/Montmorillonite Clay Multilayer-Coated Paperboards with High Barrier Properties. *Ind. Crops Prod.* **2013**, *51*, 1–6. [CrossRef]
22. Aulin, C.; Gällstedt, M.; Lindström, T. Oxygen and Oil Barrier Properties of Microfibrillated Cellulose Films and Coatings. *Cellulose* **2010**, *17*, 559–574. [CrossRef]
23. Galizia, M.; Chi, W.S.; Smith, Z.P.; Merkel, T.C.; Baker, R.W.; Freeman, B.D. 50th Anniversary Perspective: Polymers and Mixed Matrix Membranes for Gas and Vapor Separation: A Review and Prospective Opportunities. *Macromolecules* **2017**, *50*, 7809–7843. [CrossRef]
24. Andersson, C.; Ernstsson, M.; Järnström, L. Barrier Properties and Heat Sealability/Failure Mechanisms of Dispersion-Coated Paperboard. *Packag. Technol. Sci.* **2002**, *15*, 209–224. [CrossRef]
25. Zhu, Y.D.; Allen, G.C.; Adams, J.M.; Gittins, D.I.; Hooper, J.J.; Skuse, D.R. Barrier Properties of Latex/Kaolin Coatings. *Polym. Chem.* **2013**, *4*, 4386. [CrossRef]
26. Vähä-Nissi, M.; Kervinen, K.; Savolainen, A.; Egolf, S.; Lau, W. Hydrophobic Polymers as Barrier Dispersion Coatings. *J. Appl. Polym. Sci.* **2006**, *101*, 1958–1962. [CrossRef]
27. Zhu, Y.; Bousfield, D.; Gramlich, W.M. The Influence of Pigment Type and Loading on Water Vapor Barrier Properties of Paper Coatings before and after Folding. *Prog. Org. Coat.* **2019**, *132*, 201–210. [CrossRef]
28. Al-Gharrawi, M.; Ollier, R.; Wang, J.; Bousfield, D.W. The Influence of Barrier Pigments in Waterborne Barrier Coatings on Cellulose Nanofiber Layers. *J. Coat. Technol. Res.* **2022**, *19*, 3–14. [CrossRef]
29. Rämänen, P.; Pitkänen, P.; Jämsä, S.; Maunu, S.L. Natural Oil-Based Alkyd-Acrylic Copolymers: New Candidates for Barrier Materials. *J. Polym. Environ.* **2012**, *20*, 950–958. [CrossRef]
30. Lopes, C.M.A.; Felisberti, M.I. Composite of Low-Density Polyethylene and Aluminum Obtained from the Recycling of Postconsumer Aseptic Packaging. *J. Appl. Polym. Sci.* **2006**, *101*, 3183–3191. [CrossRef]
31. Şahin, G.G.; Karaboyacı, M. Process and Machinery Design for the Recycling of Tetra Pak Components. *J. Clean. Prod.* **2021**, *323*, 129186. [CrossRef]
32. Del Curto, B.; Barelli, N.; Profaizer, M.; Farè, S.; Tanzi, M.C.; Cigada, A.; Ognibene, G.; Recca, G.; Cicala, G. Poly-Paper: A Sustainable Material for Packaging, Based on Recycled Paper and Recyclable with Paper. *J. Appl. Biomater. Funct. Mater.* **2016**, *14*, 490–495. [CrossRef] [PubMed]
33. Bakker, S.; Bosveld, L.; Metselaar, G.A.; Esteves, A.C.C.; Schenning, A.P.H.J. Understanding and Improving the Oil and Water Barrier Performance of a Waterborne Coating on Paperboard. *ACS Appl. Polym. Mater.* **2022**, *4*, 6148–6155. [CrossRef] [PubMed]
34. Bakker, S.; Aarts, J.; Esteves, A.C.C.; Metselaar, G.A.; Schenning, A.P.H.J. Water Barrier Properties of Resin-Stabilized Waterborne Coatings for Paperboard. *Macromol. Mater. Eng.* **2022**, *307*, 2100829. [CrossRef]
35. Siddiq, M.; Tam, K.C.; Jenkins, R.D. Dissolution Behaviour of Model Alkali-Soluble Emulsion Polymers: Effects of Molecular Weights and Ionic Strength. *Colloid Polym. Sci.* **1999**, *277*, 1172–1178. [CrossRef]
36. Lopes Brito, E.; Ballard, N. Film Formation of Alkali Soluble Resin (ASR) Stabilized Latexes. *Prog. Org. Coat.* **2021**, *159*, 106444. [CrossRef]
37. Steward, P.A.; Hearn, J.; Wilkinson, M.C. An Overview of Polymer Latex Film Formation and Properties. *Adv. Colloid Interface Sci.* **2000**, *86*, 195–267. [CrossRef] [PubMed]
38. Keddie, J.L. Film Formation of Latex. *Mater. Sci. Eng. R Rep.* **1997**, *21*, 101–170. [CrossRef]
39. Winnik, M.A. Latex Film Formation. *Curr. Opin. Colloid Interface Sci.* **1997**, *2*, 192–199. [CrossRef]
40. Routh, A.F.; Russel, W.B. Process Model for Latex Film Formation: Limiting Regimes for Individual Driving Forces. *Langmuir* **1999**, *15*, 7762–7773. [CrossRef]
41. Badía, A.; Barandiaran, M.J.; Leiza, J.R. Biobased Alkali Soluble Resins Promoting Supramolecular Interactions in Sustainable Waterborne Pressure-Sensitive Adhesives: High Performance and Removability. *Eur. Polym. J.* **2021**, *144*, 110244. [CrossRef]
42. Helmenstine, A.M. The Chemical Composition of Air. Available online: https://www.thoughtco.com/chemical-composition-of-air-604288 (accessed on 21 October 2022).
43. Guo, Y.H.; Li, S.C.; Wang, G.S.; Ma, W.; Huang, Z. Waterborne Polyurethane/Poly(n-Butyl Acrylate-Styrene) Hybrid Emulsions: Particle Formation, Film Properties, and Application. *Prog. Org. Coat.* **2012**, *74*, 248–256. [CrossRef]
44. Wang, H.; Fan, J.; Fei, G.; Lan, J.; Zhao, Z. Preparation and Property of Waterborne UV-Curable Chain-Extended Polyurethane Surface Sizing Agent: Strengthening and Waterproofing Mechanism for Cellulose Fiber Paper. *J. Appl. Polym. Sci.* **2015**, *132*, 1–11. [CrossRef]

45. Yook, S.; Park, H.; Park, H.; Lee, S.Y.; Kwon, J.; Youn, H.J. Barrier Coatings with Various Types of Cellulose Nanofibrils and Their Barrier Properties. *Cellulose* **2020**, *27*, 4509–4523. [CrossRef]
46. Yan, X.; Ji, Y.; He, T. Synthesis of Fiber Crosslinking Cationic Latex and Its Effect on Surface Properties of Paper. *Prog. Org. Coat.* **2013**, *76*, 11–16. [CrossRef]
47. Parry, R.T. (Ed.) *Principles and Applications of Modified Atmosphere Packaging of Foods*; Springer: New York, NY, USA, 1993; ISBN 978-1-4613-5892-3.
48. Kloos, J.; Jansen, N.; Houben, M.; Casimiro, A.; Lub, J.; Borneman, Z.; Schenning, A.P.H.J.; Nijmeijer, K. On the Order and Orientation in Liquid Crystalline Polymer Membranes for Gas Separation. *Chem. Mater.* **2021**, *33*, 8323–8333. [CrossRef] [PubMed]
49. Ismail, A.F.; Khulbe, K.C.; Matsuura, T. *Gas Seperation Membranes-Polymeric and Inorganic*; Springer: New York, NY, USA, 2015; ISBN 9783319010946.
50. Wijmand, J.G.; Baker, R.W. The Solution-Diffusion Model: A Review. *J. Memb. Sci.* **1993**, *107*, 1–21. [CrossRef]
51. Koros, W.J.; Fleming, G.K. Membrane-Based Gas Separation. *J. Memb. Sci.* **1993**, *83*, 1–80. [CrossRef]
52. Proniewicz, L.M.; Paluszkiewicz, C.; Wesełucha-Birczyńska, A.; Majcherczyk, H.; Barański, A.; Konieczna, A. FT-IR and FT-Raman Study of Hydrothermally Degradated Cellulose. *J. Mol. Struct.* **2001**, *596*, 163–169. [CrossRef]
53. Oh, S.Y.; Yoo, D.I.; Shin, Y.; Seo, G. FTIR Analysis of Cellulose Treated with Sodium Hydroxide and Carbon Dioxide. *Carbohydr. Res.* **2005**, *340*, 417–428. [CrossRef] [PubMed]